Clays and Clay Minerals, Vol. 35, No. 4, 271–280, 1987.

TRANSFORMATION OF BIRNESSITE TO BUSERITE, TODOROKITE, AND MANGANITE UNDER MILD HYDROTHERMAL TREATMENT

D. C. GOLDEN, C. C. CHEN, AND J. B. DIXON

Department of Soil & Crop Sciences, Texas A&M University
College Station, Texas 77843

Abstract—Investigations were conducted to determine the hydrothermal transformations of synthetic birnessite exchanged with different metal ions. Autoclaving in a Teflon-lined stainless steel pressure vessel at 155°C for 24 hr of Mg-, Ca-, La-, and Co-saturated birnessite yielded manganese minerals having 10-Å X-ray powder diffraction (XRD) spacings. The autoclaved Mg-birnessite yielded a mineral identical to natural todorokite in its infrared (IR) spectrum and XRD patterns. High-resolution transmission electron microscopy (HRTEM) provided images having 10-, 12.5-, 15-, and 20-Å wide fringes indicating heterogeneous channel widths in the crystallographic *a* direction, and IR spectroscopy produced bands at 757, 635, 552, 515, 460, and 435 cm^{-1}, confirming the product obtained by autoclaving Mg-birnessite to be todorokite. Prolonged autoclaving of Mg-birnessite yielded manganite (γ-MnOOH) as a by-product; manganite did not form when the autoclaving time was shortened to 8 hr. Also, when Ca-saturated samples were autoclaved, the product gave d-values of 10 Å, but the XRD lines were broad and heterogeneity of the channel sizes was evident from HRTEM observations. The Ca-derivative had an IR spectrum similar to that of natural todorokite. Images showing 10-Å lattice fringes were observed by HRTEM for the Ni-saturated sample, which also produced an XRD pattern similar to that of the Mg-saturated sample. Co- and La-saturated samples did not form todorokite, although HRTEM of La-saturated samples indicated some 10-Å lattice fringes that were unstable in the electron beam. Birnessite saturated with Na, K, NH_4, Cs, Ba, or Mn(II) gave products having 7-Å spacings upon autoclaving.

Key Words—Birnessite, Buserite, High-resolution transmission electron microscopy, Hydrothermal, Manganite, Todorokite.

INTRODUCTION

Na-birnessite is a stable, layer-structure manganese oxide in which the Na can be replaced by many other cations. The structure of Na-birnessite probably consists of sheets of [MnO_6] octahedra separated by exchangeable Na and water. The basal spacings of this mineral may be 7 Å (birnessite, having a single layer of H_2O) or 10 Å (buserite, having a double layer of H_2O), depending on the number of water layers separating the octahedral sheets (Potter and Rossman, 1979). According to Turner and Buseck's (1981) nomenclature system, birnessite and buserite are the sheet-structure end members of the hollandite-romanechite [T(2, n)] and todorokite [T(3, n)] families, respectively, of the tunnel-structure manganese oxide minerals. T(2, n) stands for tunnels made of 2 × n octahedra, and T(3, n) stands for tunnels made of 3 × n octahedra (3 and 2 represent the common dimensions; n represents the variable dimension). Dry heating of K- and Ba-saturated birnessite [T(2, ∞)] gives rise to cryptomelane and hollandite, respectively (Giovanoli and Balmer, 1981; Giovanoli, 1980; Chen *et al.*, 1986) which represent T(2, 2) members of the T(2, n) family. The relevant mineralogical properties of the minerals concerned are given in Table 1. When birnessite transforms to a tunnel-structure mineral, the initial distance between the birnessite layers seems to have some control on the dimensions of the tunnel.

Certain cations, such as Mg, Ni, and Ca, are known to expand birnessite to buserite (Golden *et al.*, 1986b), and high relative humidity (RH) stabilizes this phase. Na-birnessite has a 7-Å basal spacing at low RH and a 10-Å spacing at high RH (Wadsley, 1950; Tejedor-Tejedor and Paterson, 1979). If the initial layer spacing influences the final product, the members of the todorokite family [T(3, n)] should form from buserite [T(3, ∞)]. Water saturation and cations favoring the buserite structure should be considered in such a transformation. The cationic composition of todorokite was reported by Turner (1982) on the basis of electron microprobe analysis. Therefore, their ease of forming buserite and their presence in natural todorokite were the criteria used to select cations for saturating birnessite in this study. Todorokite and birnessite are important minerals in terrestrial (Chukhrov and Gorshkov, 1981) and marine manganese nodules (Burns and Burns, 1977). Therefore, the transformation of birnessite into tunnel-structure minerals of the hollandite-romanechite group or of the todorokite group is of special interest to earth scientists, as it may provide clues to the formation of these materials in nature.

This investigation was carried out to study the effect

Table 1. Manganese oxide mineral birnessite and its transformation products.[1]

Mineral	Formula	Crystal system (space group)	Cell parameters (Å)	Tunnel size[2]
Synthetic birnessite (7-Å manganite)	$Na_4Mn_{14}O_{27}\cdot 9H_2O$	Orthorhombic	$a_0 = 8.54$; $b_0 = 5.28$ $c_0 = 14.26$	2 × 2
Hollandite	$(Ba,K)_{1-2}Mn_8O_{16}\cdot xH_2O$	Tetragonal ($I4/m$)	$a_0 = 9.96$; $c_0 = 2.86$	2 × 2
Cryptomelane	$K_{1-2}Mn_8O_{16}\cdot xH_2O$	Tetragonal ($I4/m$)	$a_0 = 9.84$; $c_0 = 2.86$	2 × 2
Todorokite (10-Å manganite)	(Na,Ca,K,Ba,Mn^{2+}) $Mn_3O_7\cdot xH_2O$	Monoclinic	$a_0 = 9.75$; $b_0 = 2.849$ $c_0 = 9.59$; $\beta = 90°$	3 × 3
Manganite	γ-MnOOH	Monoclinic	$a_0 = 8.98$; $b_0 = 5.28$ $c_0 = 5.71$; $\beta = 90°$	n.a.

[1] Mineralogical data from Burns and Burns (1977).
[2] Numbers refer to the widths of $[MnO_6]$ octahedral chains forming each side of the tunnel. n.a. = not applicable.

of cations on the transformation of birnessite under mild hydrothermal conditions to form tunnel-structure manganese oxide minerals.

EXPERIMENTAL

Preparation of Na-birnessite

Birnessite was synthesized using a modification of the procedure of Stähli (1968). Two hundred milliliters of 0.5 M $MnCl_2$ was placed in a 500-ml plastic beaker, and oxygen was bubbled through it at 22°C via a glass frit at a rate ≥1.5 liter/min. A cold (7°C) solution of 55 g of NaOH in 250 ml of H_2O was added quickly. After 5 hr, the oxygenation was stopped, and the black precipitate was dialyzed, freeze-dried, and stored in an air-tight bottle. The black precipitate of Na-buserite dehydrated during the freeze-drying procedure to form Na-birnessite (see Golden *et al.*, 1986b), the identity of which was confirmed by X-ray powder diffraction and infrared spectroscopic analyses.

Cation saturation and hydrothermal treatment

Twenty-five milligrams of the above (Na-birnessite) was shaken with 20 ml each of 1 M $MgCl_2$, $CaCl_2$, $CoCl_2$, $NiCl_2$, KCl, NH_4Cl, CsCl, $LaCl_3$, or $BaCl_2$ solutions in duplicate for 12 hr at 22°C to saturate the birnessite with each of these cations. One set of replicates was washed four times with 20-ml portions of distilled deionized water and freeze-dried. The freeze-dried residues were dissolved in a HCl:$NH_2OH\cdot HCl$ mixture as described below under analytical methods, and the digestates were analyzed for Na, Mn, and the respective saturating cation. The extent of saturation was determined from these analyses by assuming Na to be the only exchange cation on the original Na-birnessite and the saturating cation to replace this Na to varying degrees, using the relation:

$$\% \text{ saturation} = (P_m \times Z)100/[P_{Na} + (P_m \times Z)],$$

where P_m is the atom percent of saturating cation of valence Z, and P_{Na} is the atom percent of Na in M-exchanged Na-birnessite.

Washed samples of the second set of replicates were autoclaved at 155°C in Teflon-lined, sealed, stainless steel containers (25 ml) under autogenous pressure for 24 hr. The containers were cooled to room temperature, and the contents were washed free of excess salt. The products were freeze-dried and stored.

Analytical methods

X-ray powder diffraction analyses (XRD) were carried out on random and oriented powder mounts in a Philips Norelco X-ray diffractometer equipped with a graphite monochromator and using CuKα radiation. Expandability of the samples was tested by XRD following intercalation of n-alkylammonium ions (Golden *et al.*, 1986b). Samples were examined by transmission electron microscopy using a Zeiss 10C electron microscope operated at 60–100 kV. The washed samples were dispersed in distilled water and sonicated prior to deposition on a holey carbon film. Infrared (IR) spectroscopy was performed on 300-mg KBr pellets containing about 0.3 mg of the oxide pressed at 1.38×10^5 kPa for 5 min. Spectra were recorded using a Perkin Elmer 283 IR spectrometer equipped with a Model 3500 data station.

Mn and Mg were determined on 50-mg samples digested in 6 M HCl and 2 ml of 0.1 N $NH_2OH\cdot HCl$/0.1 N HNO_3. Digestates were made to 100 ml in a volumetric flask and diluted before analysis. The oxidation state of Mn in todorokite was determined by the oxalic acid-permanganate back-titration procedure of Piper *et al.* (1984).

RESULTS

Synthetic Na-birnessite

The synthetic Na-birnessite product was composed of plates of roughly hexagonal shape and a few lath-shaped particles (Figures 1a and 1b). The samples of Na-birnessite after cation saturation showed two types of basal spacings at 54% relative humidity (RH) prior to autoclaving. Mg-, Ni-, Ca-, and La-saturated birnessite gave basal spacings of 10 Å, whereas birnessite saturated with other cations had a 7-Å spacing in accord with earlier observations (Tejedor-Tejedor and Paterson, 1979; Golden *et al.*, 1986b). The exchangeability of Ca, Ni, NH_4, K, and Mn for Na was 100%,

https://doi.org/10.1346/CCMN.1987.0350404 Published online by Cambridge University Press

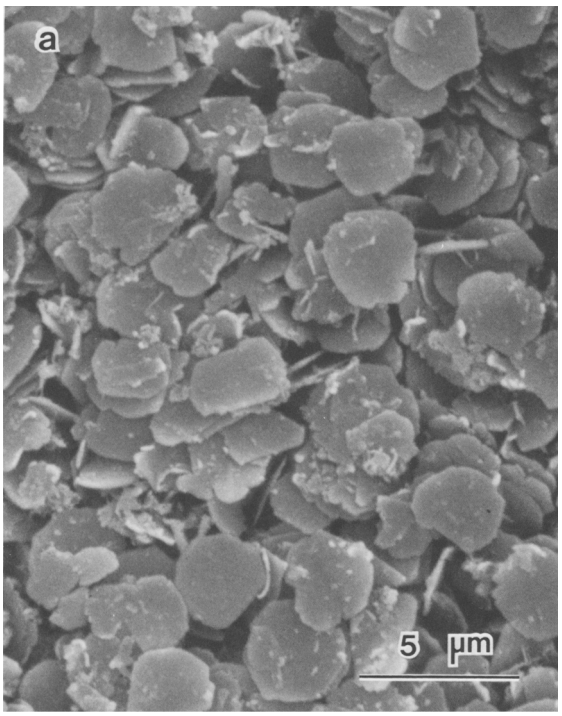

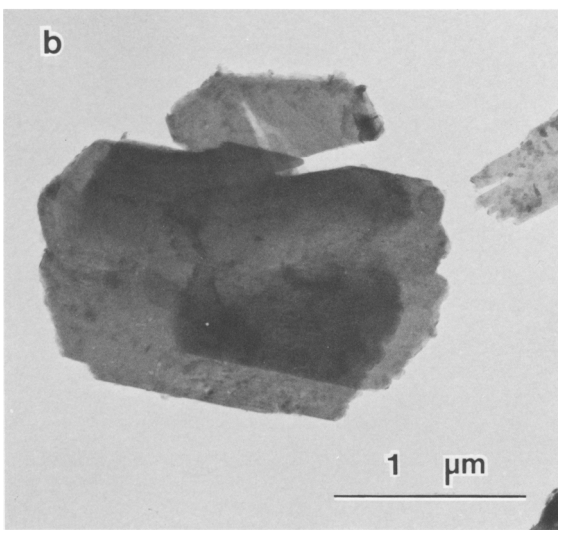

Figure 1. (a) Scanning electron micrograph of synthetic birnessite. (b) Transmission electron micrograph of platy birnessite particles.

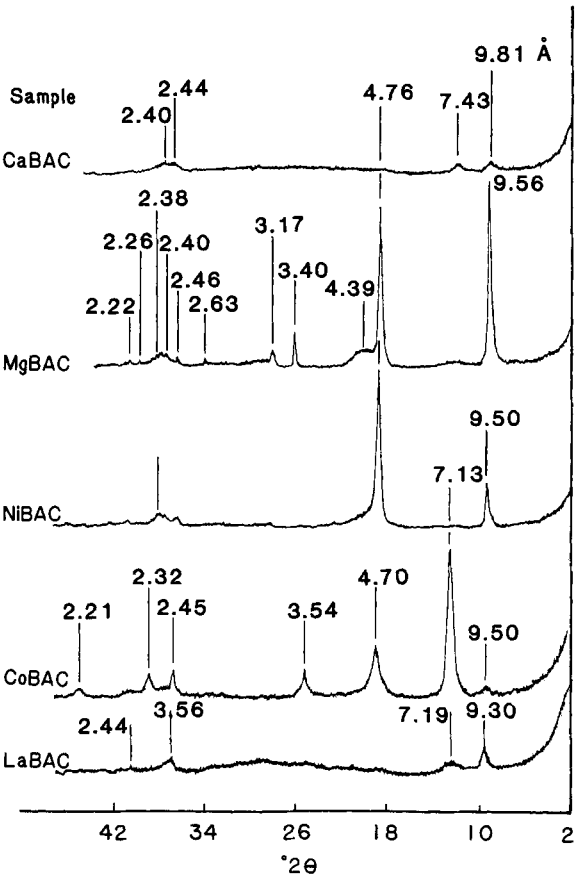

Figure 2. X-ray powder diffraction patterns of autoclaved samples of Ca- (CaBAC), Mg- (MgBAC), Ni- (NiBAC), Co- (CoBAC), and La-saturated birnessite (LaBAC). (CuKα radiation.)

but other cations were less effective in replacing Na (e.g., Cs, 99%; Mg, 96%; Ba, 94%; Co, 89%; and La, 45%). Some Mn was released by Ni (0.2%) and Co (1.9%).

X-ray powder diffraction of autoclaved birnessite

XRD curves of the autoclaved cation-saturated birnessites (Figures 2 and 3) showed the same basal spacings (7- or 10-Å) as did the birnessites prior to autoclaving; however, the relative intensities of the peaks were different and additional peaks were present. Ca-birnessite, after autoclaving, gave an XRD pattern (Figure 2, sample CaBAC) having broad, low-intensity peaks at 9.81, 7.43, 2.44, and 2.40 Å. The 9.81- and 7.43-Å peaks had the same intensity. The Mg-saturated birnessite, after autoclaving, gave sharp, intense XRD peaks of todorokite (Figure 2, sample MgBAC), and two peaks at 3.40 and 2.25 Å due to manganite (γ-MnOOH). Ni-birnessite also gave a 9.5-Å basal spacing, but the second order peak at 4.75 Å was much more intense than that at 9.5 Å (Figure 2, sample NiBAC). The Co-birnessite showed XRD peaks at 9.5 and 7.13 Å. The second order peak of the 9.5-Å reflection was more intense than the 9.5-Å peak itself. The autoclaved Na-, K-, NH_4-, Cs-, Ba-, and Mn(II)-birnessites all had a basal peak at 7 Å (Figure 3). K-birnessite had additional broad peaks at 4.95, 3.52, 3.13, and 2.40 Å. Most of the Mn-birnessite when autoclaved transformed to manganite as indicated by the XRD peaks at 3.41, 2.64, 2.52, and 2.41 Å.

The n-alkylammonium compounds did not inter-

https://doi.org/10.1346/CCMN.1987.0350404 Published online by Cambridge University Press

calate any of the products obtained by autoclaving the cation-saturated birnessite.

Infrared spectroscopy

IR analysis was performed on all samples having 10-Å spacings (Figure 4). The IR spectra of the products formed by autoclaving Ca- (sample CaBAC) and Mg- (sample MgBAC) saturated birnessite were similar to that of todorokite from Charco Redondo, Cuba (sample TCRC), indicating the samples to be todorokite. The products formed by autoclaving Ni-saturated birnessite (sample NiBAC) also yielded a spectrum similar to that of todorokite; however, in the latter sample the band at 515 cm^{-1} was more intense and the bands at 435 and 552 cm^{-1} were relatively smaller compared to those in the spectrum of sample TCRC.

The autoclaved product from Co-saturated birnessite (sample CoBAC), yielded an IR pattern with peaks at 495, 645, 1110, and 1122 cm^{-1}. This spectrum was different from that of todorokite due to the absence of distinct bands at 755 and 555 cm^{-1} and also by the presence of two sharp bands at 1122 and 1110 cm^{-1}. Also, the CoBAC absorbance at 435 cm^{-1} was broader than for any other sample.

High-resolution transmission electron microscopy (HRTEM)

The samples obtained by autoclaving Ca-, Mg-, Ni-, Co-, and La-birnessite were examined by HRTEM because the XRD pattern of these samples had a 10-Å d spacing. The product obtained by autoclaving Ca-birnessite consisted of fibers twinned at 120° to each other (Figures 5a and 5b). Three sets of fibers were twinned at 120° to give rise to a trilling network similar to that of todorokite. The heterogeneity of tunnel dimensions in the *a* direction can be observed in Figure 5b from the lattice fringes. Fringe dimensions which indicate tunnel widths in the *a* direction were predominantly 7.5, 10, 12.5, and 15 Å, respectively, corresponding to 2, 3, 4, and 5 octahedral ribbon widths. The product obtained by autoclaving Mg-birnessite also consisted of thin fibers twinned at 120°, similar to those of natural todorokite (Figures 5c, 5d, and 5g). HRTEM of the product obtained by autoclaving Mg-birnessite indicated lattice fringes mainly of 10-Å in the *a* direction plus 12.5-, 15-, and 20-Å fringes. Trilling morphology in the product obtained by autoclaving Mg-birnessite was observed mainly near the original birnessite plate, whereas single fibers were noted extending from this central region. Lattice fringes of the single fibers extending from the product obtained by autoclaving Mg-birnessite were predominantly 10 Å, indicating a uniform channel dimension in the *a* direction (Figure 5e).

The product obtained by autoclaving Mg-birnessite contained a second phase, manganite (determined by XRD), in minor quantities. Manganite formed large lath-shaped crystals which were twinned at 120° (Figure 5f). The product obtained by autoclaving Ni-saturated birnessite contained two morphologically distinct types of particles: fibers having lattice fringes comparable to todorokite (Figure 6b) and electron-dense hexagonal plates (Figure 6a); however, XRD and IR data did not indicate two distinct minerals. The products obtained by autoclaving Co-birnessite (Figures 6c and 6d) were similar in morphology and XRD to the original birnessite (Figure 1), and gave little morphological evidence for formation of todorokite. For the product obtained by autoclaving La-birnessite, lattice fringes observed by HRTEM were not stable under the electron beam and could not be recorded photographically (Figures 6e and 6f).

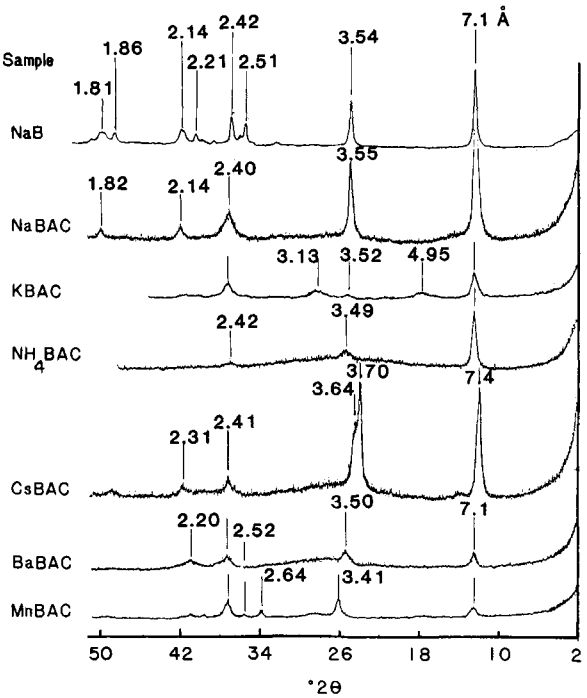

Figure 3. X-ray powder diffraction patterns of Na-birnessite prior to autoclaving (NaB) and of autoclaved Na- (NaBAC), K- (KBAC), NH_4^+- (NH_4BAC), Cs- (CsBAC), Ba- (BaBAC), and Mn(II)-saturated birnessite (MnBAC). (CuKα radiation.)

Electron diffraction

Electron diffraction patterns (ED) of the samples exhibiting 10-Å spacings (Figure 7) provided additional information supporting the above observations. Inasmuch as the crystals in samples CaBAC, MgBAC, NiBAC, and LaBAC were twinned at 120° angle (Figures 5, 6a, 6b, 6e, and 6f) the ED was the result of a composite of three twinned crystals having a^* dimensions 120° from each other. (Electron diffraction of sample CoBAC showed no evidence for twinned crystals or heterogeneous channel sizes.) The ED pattern

https://doi.org/10.1346/CCMN.1987.0350404 Published online by Cambridge University Press

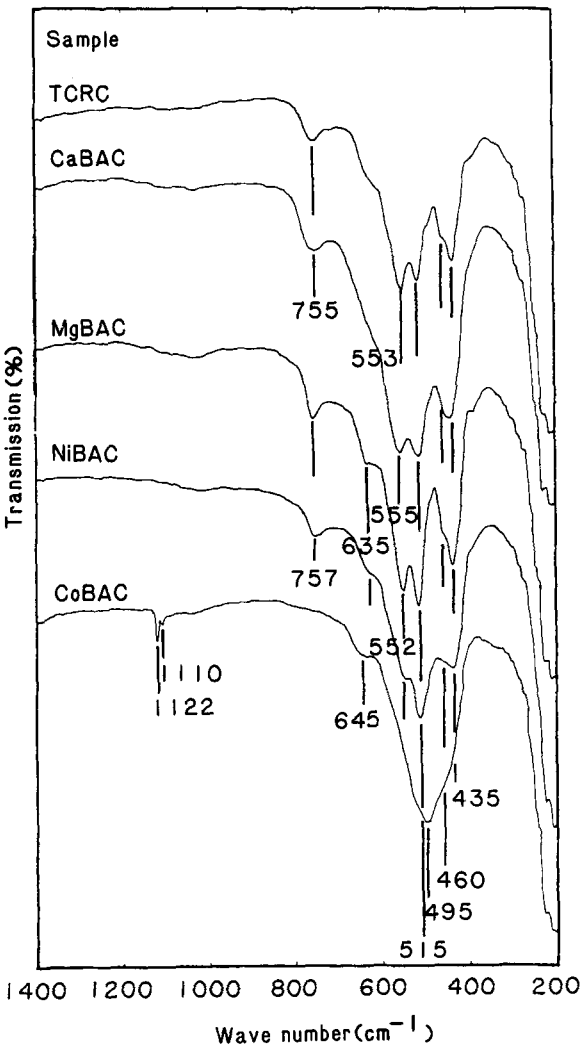

Figure 4. Infrared spectra of natural todorokite (TCRC); autoclaved Ca-birnessite (CaBAC); autoclaved Mg-birnessite (MgBAC); autoclaved Ni-birnessite (NiBAC); and autoclaved Co-birnessite (CoBAC).

for Na-birnessite was indexed assuming an orthorhombic unit cell (Figure 7f). A characteristic streaking due to the heterogeneity of channel size is seen for all the tunnel-structure minerals examined (Figures 7a, 7b, 7c, and 7e). Streaked spots due to larger channel sizes were noted as well for sample LaBAC (15 Å), sample CaBAC (12.5 Å), and sample MgBAC (12.5, 15, and 17.5 Å). Multiple channel widths are most evident in the ED patterns of sample LaBAC. The diffracting crystal in sample NiBAC produced only a few spots, probably due to tilting of the particle, yet it showed streaking similar to that in ED patterns from samples MgBAC and CaBAC.

Chemical analysis

Chemical analysis was performed on birnessite and autoclaved Mg-birnessite (todorokite) only. The analyses of Mg and Mn for these samples and determined oxidation numbers are given in Table 2. The total Mn in the natural samples is similar to that of synthetic todorokite (53.7%). Also, the atomic ratio Mn:Mg of the synthetic sample corresponds closely to the atomic ratio Mn:Σ Mg, Ca, Ba, Na, K of the natural samples.

The total Mg was the largest in the synthetic sample of todorokite, as expected, because Mg was the only cation other than Mn introduced during the synthesis. For the natural samples, the Mn : other cations atomic ratio (i.e., other cations as M^{2+} ions) fluctuated around an average value of 6.72:1, which is similar to that of the synthetic sample. Synthetic birnessite showed a slightly lower oxidation number for Mn than did todorokite.

DISCUSSION

The broad, low intensity XRD peaks for the product obtained by autoclaving Ca-birnessite indicate either small particle size, a high degree of disorder in the crystallites, or both. XRD alone, however, cannot distinguish between different forms of 10-Å manganese oxide minerals (Burns *et al.*, 1983), and the identity of todorokite and buserite continues to be a subject of controversy (Giovanoli, 1985; Burns *et al.*, 1985). Several recent HRTEM observations of todorokite subsequent to the work of Giovanoli (1980), which were not considered in his review (Giovanoli, 1985), suggest a structural model containing 3 × 3 tunnels. For todorokite from continental (Turner and Buseck, 1981) and marine manganese nodules (Turner and Buseck, 1982; Turner *et al.*, 1982; Siegel and Turner, 1983) a tunnel structure containing "walls" of triple chains of edge-shared [MnO_6] octahedra and "floors" and "ceilings" of edge-shared [MnO_6] octahedra, most commonly three octahedra wide, was inferred. Burns *et al.* (1985) further showed that the (3 × 3) tunnel structure agrees well with the IR data reported by Potter and Rossman (1979), which, as interpreted above, favor a layer structure. The IR spectrum of Ca-birnessite is very similar to that of natural todorokite, although the bands are less sharp compared to those of the todorokite reference material from Charco Redondo, Cuba (sample TCRC). HRTEM images suggest the presence of tunnels of variable dimension in the *a* direction, which may explain the disorder indicated by broad, weak XRD peaks. The above evidence and the inability of n-alkylammonium compounds to intercalate autoclaved products of Ca-birnessite indicate a mineral similar to todorokite. The product obtained by autoclaving Mg-birnessite produced sharp, intense XRD peaks and IR bands indicating better crystalline order than that of the product obtained by autoclaving Ca-birnessite. According to Potter and Rossman (1979), IR spectroscopy yields a more complete and reliable description of manganese oxide materials than does XRD. The IR spectrum of the product obtained by

https://doi.org/10.1346/CCMN.1987.0350404 Published online by Cambridge University Press

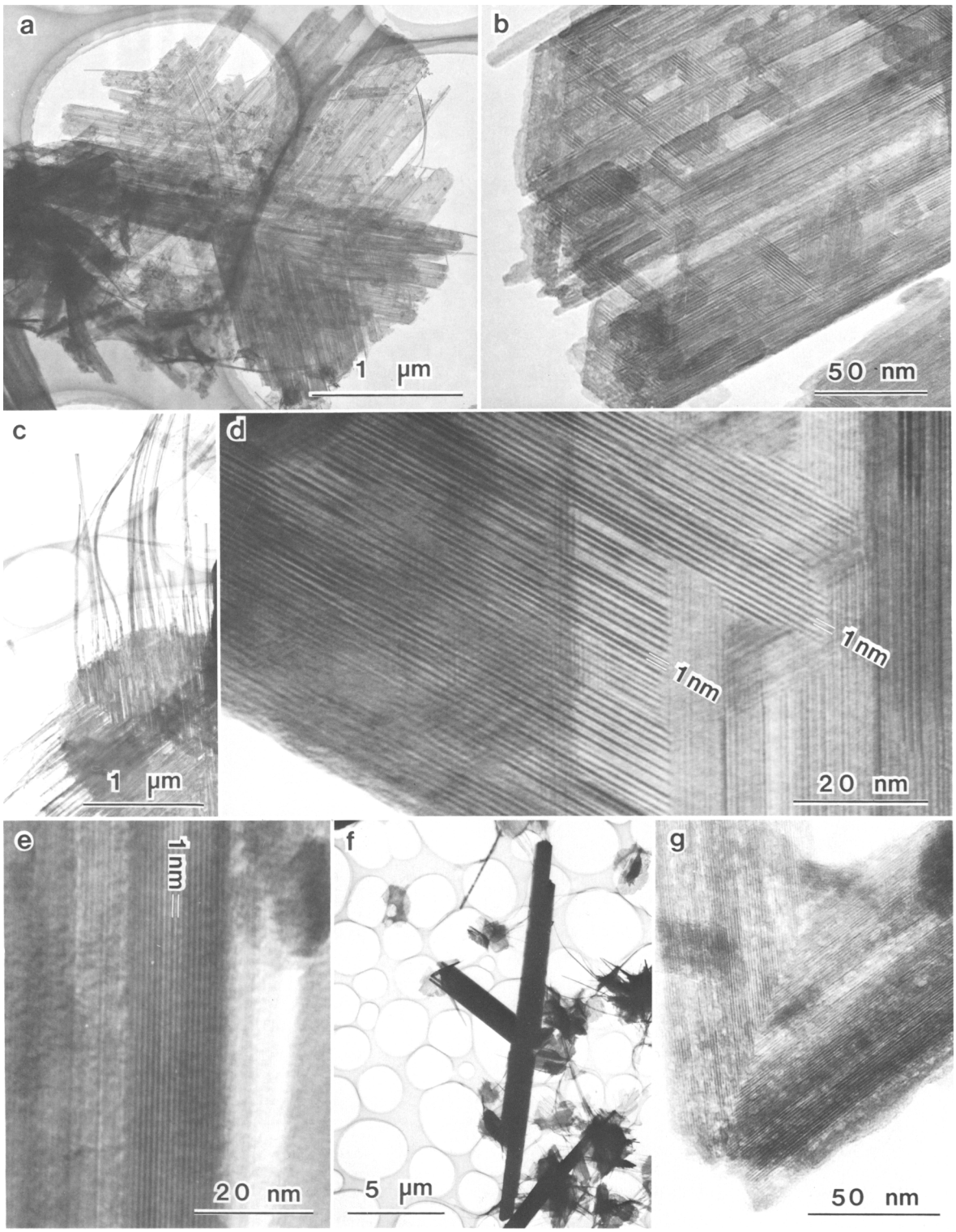

Figure 5. Transmission electron microscopy images of autoclaved samples of birnessites saturated with: Ca (a, b), Mg (c, d, e, f). (g) High-resolution transmission electron image of natural todorokite from Montenegro Mine, Cuba. (1 nm = 10 Å.)

https://doi.org/10.1346/CCMN.1987.0350404 Published online by Cambridge University Press

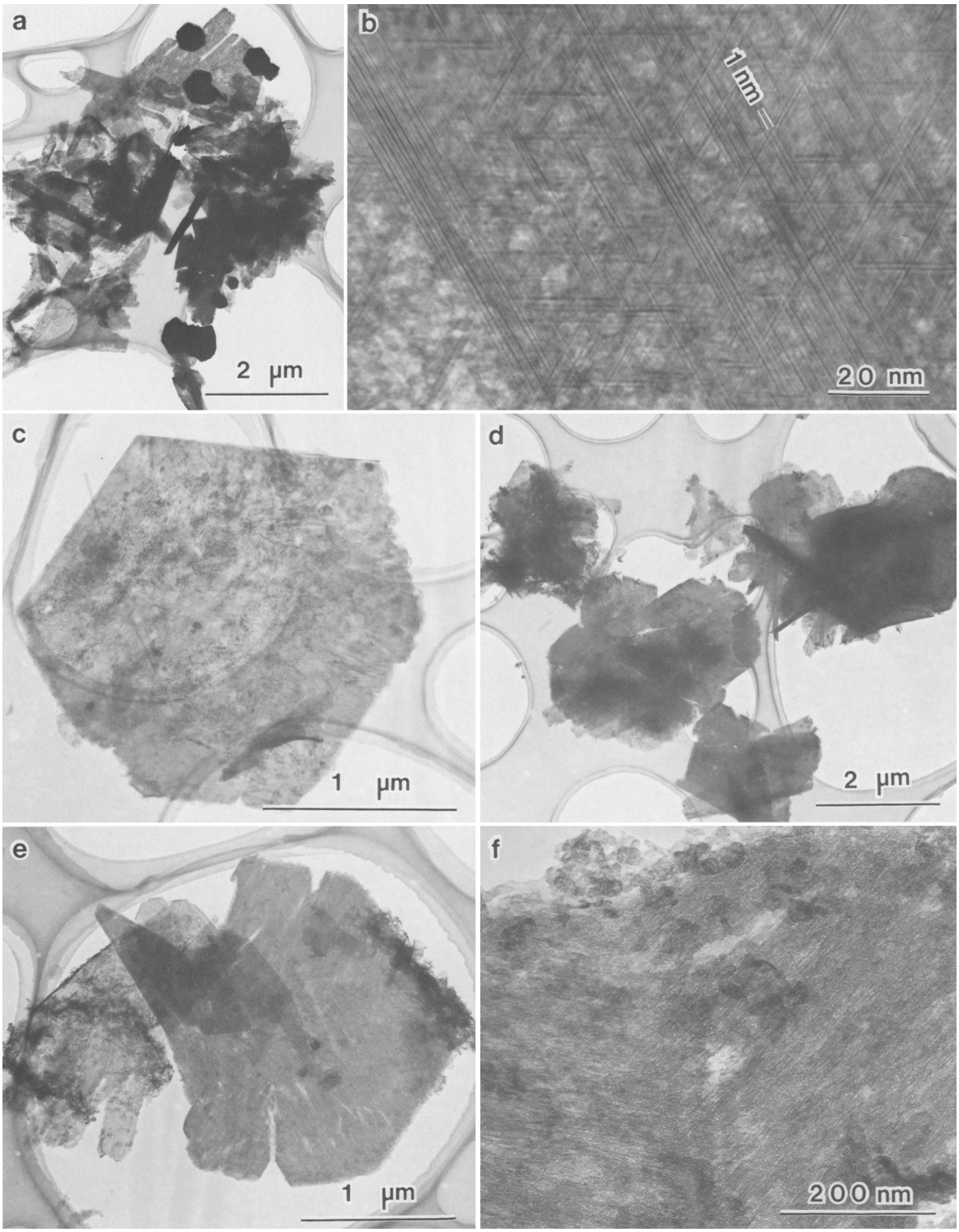

Figure 6. Transmission electron microscopy images of autoclaved samples of cation-saturated birnessite: Ni (a, b), Co (c, d), and La (e, f).

https://doi.org/10.1346/CCMN.1987.0350404 Published online by Cambridge University Press

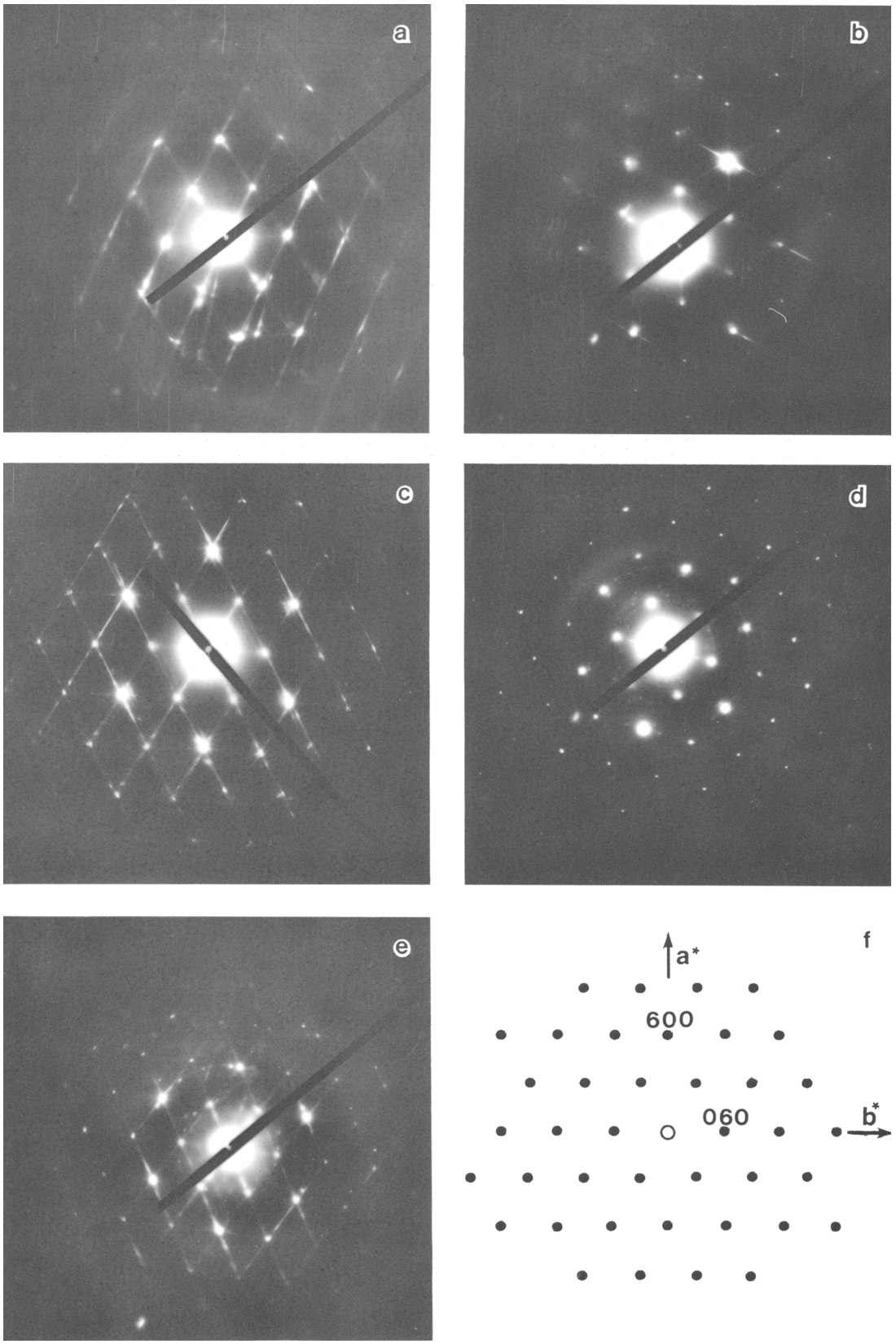

Figure 7. Electron diffraction patterns of: (a) product obtained by autoclaving Ca-birnessite, (b) product obtained by autoclaving Ni-birnessite, (c) product obtained by autoclaving Mg-birnessite, (d) product obtained by autoclaving Co-birnessite, and (e) product obtained by autoclaving La-birnessite. (f) Indexed electron diffraction pattern of Na-birnessite.

https://doi.org/10.1346/CCMN.1987.0350404 Published online by Cambridge University Press

Table 2. Chemical analysis of natural and synthetic todorokites and synthetic birnessite.[1]

Sample	Mn (%)	Mg (%)	Mn : other cations[2] (as divalent cations) atom ratio	Average oxidation states of Mn
Synthetic todorokite[3]	53.70	3.56	6.67:1	3.620
Synthetic birnessite	41.32	—	7.00:1	3.571
Charco Redondo, Cuba[4,6]	52.98	1.96	6.52:1	3.659
Ferragudo, Portugal[4,6]	53.05	2.35	6.87:1	3.673
Hüttenberg, Austria[4,6]	52.02	1.28	7.94:1	3.743
Tarantana, Cuba[5,6]	52.46	2.11	6.69:1	3.738
Charco Redondo, Cuba[5,6]	51.55	1.94	6.14:1	3.679
Ponupo, Cuba[5,6]	51.58	0.53	6.00:1	3.661
Charco Redondo, Cuba[5,6]	53.74	1.89	6.94:1	3.580
Average for natural todorokite	52.48 (0.82)	1.72	6.72:1	3.676 (0.054)

[1] Values in parenthesis indicate standard deviation.
[2] Includes Ca, Sr, Ba, Na, K, and Mg; Co and Ni values were negligible.
[3] Average of four determinations.
[4] Values calculated from Frondel *et al.* (1960).
[5] Values calculated from Straczek *et al.* (1960).
[6] Natural todorokite.

autoclaving Mg-birnessite is identical to that of sample TCRC, indicating it to be todorokite. The variability of tunnel *a* dimension as observed by HRTEM was similar to that reported for natural samples (Chukhrov *et al.*, 1979; Turner and Buseck, 1979; Turner *et al.*, 1982). The manganite impurity observed in the product obtained by autoclaving Mg-birnessite can be eliminated by employing an autoclaving time of 8 hr (Golden *et al.*, 1986a). The relatively large size of the manganite crystals confirms the formation of manganite via dissolution and reprecipitation. Formation of manganite indicates that some of the low-valence Mn ions were expelled from birnessite or todorokite to the solution during the autoclaving and reprecipitated as manganite. A coexisting manganite phase was observed for some samples of natural todorokite from Charco Redondo, Cuba (Turner, 1982).

Because Ni and Co have been reported to be associated with todorokite (Burns and Burns, 1978), they were included in these experiments. XRD data of the product obtained by autoclaving Ni-birnessite were similar to those reported for lithiophorite and asbolane (or asbolan) (Ostwald, 1984; Chukhrov *et al.*, 1980). The presence of two types of morphologies, however, indicates the possible presence of two phases. The electron-dense, hexagonal phase may be the platy mineral asbolane, which consists of $[MnO_6]$ octahedral sheets and islands of Co- or Ni-hydroxy interlayers (Chukhrov *et al.*, 1982); the phase that produced lattice fringes that indicated twinning on a micro scale at 120° is a todorokite-like phase. Such fine-scale twinning causing an apparent plate-like morphology in some todorokites was reported by Turner and Buseck (1981).

The product obtained by autoclaving Co-birnessite could not be identified from the available XRD, IR, and TEM data. No lattice fringes were detected for this material by HRTEM, indicating the probable absence of tunnels. The product obtained by autoclaving La-birnessite was a todorokite-like mineral, as inferred from HRTEM and ED data. XRD of the products obtained by autoclaving Na-, K-, NH_4-, Cs-, Ba-, or Mn-saturated birnessite indicated no 10-Å spacings.

All the products obtained by autoclaving cation-saturated birnessite (except that obtained from the Co-saturated sample) were disordered in the *a* direction, as indicated by streaking in the ED patterns. Evidence for larger tunnels was also observed in these ED patterns. The presence of fibers twinned at 120° caused the formation of pseudo hexagonal ED patterns having a^* directions 120° to each other.

Chemical analyses indicated an increase in the oxidation number of Mn from birnessite to todorokite, probably due to a disproportionation of Mn^{3+} to Mn^{4+} and Mn^{2+} and to the ejection of some Mn^{2+} into the solution during the synthesis. Prolonged autoclaving caused Mn^{2+} to react with some todorokite or unreacted birnessite to form manganite (γ-MnOOH).

CONCLUSIONS

The overall tendency for the formation of todorokite from birnessite decreased in the following order: Mg- > Ca- > Ni-birnessite. La-birnessite also showed some evidence for a tunnel-structure mineral by exhibiting poorly formed lattice fringes corresponding to an *a* dimension of 10 Å. Upon autoclaving the birnessites having stable 7-Å spacings gave rise to tunnel structures that are two octahedra wide (hollandite and cryptomelane), whereas relatively stable, 10-Å forms (buserite) favored the formation of todorokite. For autoclaved Mg-birnessite XRD peak intensities and line-widths indicated a well-crystallized sample having relatively less disorder; and the IR peaks of this material were sharp and comparable to those of well-crystallized todorokite from Charco Redondo, Cuba. The formation of todorokite-like phases from Ni-birnessite indicates the possibility of the formation of Ni-containing todorokite, in agreement with the observations of Burns and Burns (1978).

ACKNOWLEDGMENTS

The authors thank Nancy Lee for her help in preparing the manuscript and R. Giovanoli for making available to us his synthesis procedures and publications. We thank R. Giovanoli, F. A. Mumpton, and an anonymous reviewer for their helpful comments and also D. R. Velben for reviewing the final draft.

REFERENCES

Burns, R. G. and Burns, V. M. (1977) The mineralogy and crystal chemistry of deep-sea manganese nodules—A poly-

metallic resource of the twenty-first century: *Phil. Trans. Roy. Soc. London* **A.286,** 283–301.

Burns, R. G., Burns, V. M., and Stockman, H. (1983) A review of the todorokite-buserite problem: Implications to the mineralogy of marine manganese nodules: *Amer. Mineral.* **68,** 972–980.

Burns, R. G., Burns, V. M., and Stockman, H. W. (1985) The todorokite-buserite problem: Further considerations: *Amer. Mineral.* **70,** 202–204.

Burns, V. M. and Burns, R. G. (1978) Post-depositional metal enrichment processes inside manganese nodules from the north equatorial Pacific: *Earth Planet. Sci. Lett.* **39,** 341–348.

Chen, C. C., Golden, D. C., and Dixon, J. B. (1986) Transformation of synthetic birnessite to cryptomelane: An electron microscopy study: *Clays & Clay Minerals* **34,** 565–571.

Chukhrov, F. V. and Gorshkov, A. I. (1981) Iron and manganese oxide minerals in soils: *Trans. Royal Society Edinburgh* **72,** 195–200.

Chukhrov, F. V., Gorshkov, A. I., Sivtsov, A. V., and Berezovskaya, V. V. (1979) New data on natural todorokites. *Nature* **278,** 631–632.

Chukhrov, F. V., Gorshkov, A. I., Vitovskaya, I. V., Drits, V. A., and Sivtsov, A. V. (1982) On the nature of Co-Ni asbolane; a component of some supergene ores: in *Ore Genesis—The State of the Art,* G. C. Amstutz, A. El Gorezy, G. Frenzel, C. Kluth, G. Moh, A. Wauschkuhn, and R. C. Zimmerman, eds., Springer-Verlag, Berlin, 230–239.

Chukhrov, F. V., Gorshkov, A. I., Vitovskaya, I. V., Drits, V. A., Sivtsov, A. V., and Rudnitskaya, Y. S. (1980) Crystallochemical nature of Co-Ni asbolane: *Int. Geol. Rev.* **24,** 598–604.

Frondel, C., Marvin, U. B., and Ito, J. (1960) New occurrences of todorokite: *Amer. Mineral.* **45,** 1167–1173.

Giovanoli, R. (1980) On natural and synthetic manganese nodules: in *Geology and Geochemistry of Manganese,* I. M. Varentsov and G. Grasselly, eds., Akademiai Kiado, Budapest, 160–202.

Giovanoli, R. (1985) A review of the todorokite-buserite problem: Implications to the mineralogy of marine manganese nodules. Discussion: *Amer. Mineral.* **70,** 202–204.

Giovanoli, R. and Balmer, B. (1981) A new synthesis of hollandite. A possibility of immobilizing nuclear waste: *Chimia* **35,** 53–55.

Golden, D. C., Chen, C. C., and Dixon, J. B. (1986a) Synthesis of todorokite: *Science* **231,** 717–719.

Golden, D. C., Dixon, J. B., and Chen, C. C. (1986b) Ion exchange, thermal transformations, and oxidizing properties of birnessite: *Clays & Clay Minerals* **34,** 511–520.

Ostwald, J. (1984) Two varieties of lithiophorite in some Australian deposits: *Mineral. Mag.* **48,** 383–388.

Piper, D. Z., Basler, J. R., and Bischoff, J. L. (1984) Oxidation state of marine manganese nodules: *Geochim. Cosmochim. Acta* **48,** 2347–2355.

Potter, R. M. and Rossman, G. R. (1979) The tetravalent manganese oxides: Identification, hydration, and structural relationships by infrared spectroscopy: *Amer. Mineral.* **64,** 1199–1218.

Siegel, M. D. and Turner, S. (1983) Crystalline todorokite associated with biogenic debris in manganese nodules. *Science* **219,** 172–174.

Stähli, E. (1968) Über Manganate(IV) mit Schichten-Struktur: Ph.D. thesis, Univ. Bern, Bern, Switzerland, 37 pp.

Straczek, J. A., Horen, A., Ross, M., and Warshaw, C. M. (1960) Studies of the manganese oxides. IV. Todorokite: *Amer. Mineral.* **45,** 1174–1184.

Tejedor-Tejedor, M. I. and Paterson, E. (1979) Reversibility of lattice collapse in synthetic buserite: in *Proc. Int. Clay Conf., Oxford, 1978,* M. M. Mortland and V. C. Farmer, eds., Elsevier, Amsterdam, 501–508.

Turner, S. (1982) A structural study of tunnel manganese oxides by high-resolution transmission electron microscopy: Ph.D. thesis, Arizona State University, Tempe, Arizona, 239 pp.

Turner, S. and Buseck, P. R. (1979) Manganese oxide tunnel structures and their intergrowths: *Science* **203,** 456–458.

Turner, S. and Buseck, P. (1981) Todorokites: A new family of naturally occurring manganese oxides: *Science* **212,** 1024–1027.

Turner, S. and Buseck, P. R. (1982) HRTEM and EDS of tops and bottoms of some Ni-bearing Mn-nodules: *EOS* **63,** p. 1010.

Turner, S., Siegel, M. D., and Buseck, P. R. (1982) Structural features of todorokite intergrowths in manganese nodules: *Nature* **296,** 841–842.

Wadsley, A. D. (1950) A hydrous manganese oxide with exchange properties: *J. Amer. Chem. Soc.* **72,** 1782–1784.

(Received 29 April 1986; accepted 28 January 1987; Ms. 1583)